

INSTITUTE OF PLASMA PHYSICS

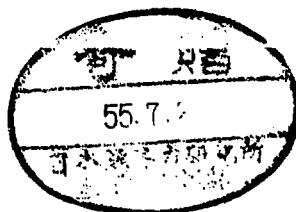
NAGOYA UNIVERSITY

A MEASUREMENT OF DEUTERIUM NEUTRAL
BY THE BALMER-SERIES
IN THE STP-2 HIGH BETA SCREW PINCH TOKAMAK

S. Yamaguchi and K. Hirano
(Received - June 12, 1980)

IPPJ- 471

June 1980



RESEARCH REPORT

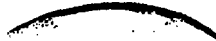
NAGOYA, JAPAN

A MEASUREMENT OF DEUTERIUM NEUTRAL
BY THE BALMER-SERIES
IN THE STP-2 HIGH BETA SCREW PINCH TOKAMAK

S. Yamaguchi and K. Hirano
(Received - June 12, 1980)

IPPJ- 471

June 1980



Further communication about this report is to be sent to the Research Information Center, Institute of Plasma Physics, Nagoya University, Nagoya 464, Japan.

ABSTRACT

The Balmer-alpha and beta are measured with a calibrated spectrograph in STP-2 screw pinch tokamak operated under the maximum toroidal field being 9.2 kG, peak plasma current 30 kA and filling pressure 5 mtorr.

The electron temperature and density profiles are obtained by ruby laser Thomson scattering. It is shown that electron temperature is about 10 eV and density is of the order of $10^{14}/\text{cm}^3$.

A non-cylindrical symmetric Abel-inversion technique is used to deduce the emission coefficient profiles from that of the line intensity of the Balmer's. In the present parameter range the neutral deuterium density is almost equal to the population density of the ground state, so that it is obtainable from measured intensities of D_{α} and D_{β} which give the population densities of the upper levels $i = 3$ and 4 .

The Collisional Radiative (CR) model is applied to the rate equations to estimate the ground state population density. It is found that at 4 μsec from the start of the discharge the deuterium neutral density may be approximately $2 \times 10^{12}/\text{cm}^3$ at the center of plasma and $2 \times 10^{14}/\text{cm}^3$ at the periphery. These values may contain an error of about factor two. Time history of neutral deuterium density is consistent with the increase of plasma density.

1. INTRODUCTION

Shock heated tokamaks or screw pinches have been studied for many years to achieve high beta plasma in toroidal field geometry at various places.⁽¹⁻³⁾ The series of STP-2 experiments have also been conducted to learn high beta plasma behavior in a tokamak-like configuration.⁽⁴⁾ It is well known in linear theta-pinch experiments that the initial ionization degree before shock compression gives important effects on the final plasma. Therefore, in this paper we tried to trace ionization or plasma build-up process through both neutral particle and usual electron density measurements. Neutral particle density has been obtained by absolute intensity measurements of the Balmer series lines of deuterium D_α and D_β , while the electron density and temperature by Thomson scattering and also by CO_2 laser interferometer. Due to very high beta value produced by shock heating STP-2 plasma does not have cylindrical symmetry to apply usual Abel inversion technique for estimating so-called emission coefficients. These difficulties are overcome using non-cylindrical symmetric Abel inversion technique developed by Matoba and Funabashi⁽⁵⁾ and extended by Miyata and Yasumoto.⁽⁶⁾ From the population density of the level with the principal quantum number $i = 3$ and 4 thus obtained, neutral deuterium density or population density of ground state is calculated under CR-model rather than usual Corona model since electron density is much higher than usual tokamak experiments.

Some discussions are given of the radiation trapping effect which may have decisive effects to estimate population density of ground state from that of upper level in the case of lower density plasmas with large volume like a large tokamak.

In Sec.2, the optical system for absolute measurement of D_α and D_β

lines is described in detail in addition to some brief explanations of STP-2 system. In Sec.3 detailed discussions are described of theoretical bases to estimate the population density of ground state from that of higher state.

2. EXPERIMENTS AND DATA PROCESSING

Figure 1 shows STP-2 device and the position of the diagnostics around the torus. The major and minor radii of the quartz tube are 25 cm and 9.5 cm, respectively. In this series of experiments the maximum plasma current and toroidal field are chosen to be 30 kA and 9.2 kG, respectively. Their typical waveforms are shown in Fig.2. These parameters are chosen so as to achieve relatively smooth plasma motion. The working deuterium gas is puff injected into the torus. The filling gas number density is fixed to $3.5 \times 10^{14}/\text{cm}^3$. The pre-ionization is done by small co-axial plasma gun followed by relatively weak Z-discharge under weak toroidal field. As a result, ionization degree of 5 to 10 % is achieved.

A schematic drawing is shown of the spectroscopic measurement system in Fig.3. The monochromator has following characteristics; focal length is 20 cm, resolution 20 \AA , and slit height 1 cm. All the optical component including lenses, optical fiber and window of the photomultiplier are made of quartz. As is shown in Fig.3, observable solid angle is 10^{-4} str which is determined by a small lens attached to the inlet end of the fiber, which has a circular cross section of 3.6 mm diameter. The outlet end has a rectangular cross section of 10 mm high and 1 mm wide. The inlet end of the fiber is placed on a plastic rail which is attached on the toroidal coil at a distance of 20 cm upward from the equatorial plane of the torus and is scanable over 13.5 cm on the rail out of 19 cm dis-

charge tube is painted black in order to avoid the stray light reflected from the discharge tube wall. An NBS standard tungsten lamp is used for the absolute intensity calibration of the whole present spectroscopic measurement system. The electron temperature and density are measured by the laser scattering system placed at $\phi = 180^\circ$ from the spectroscopic system. As usual, the laser system is calibrated by Rayleigh scattering for electron density. A CO_2 laser interferometer system at $\phi = 90^\circ$ is also used to confirm the density measurement by the scattering system.

An intensity profile of D_α line obtained is given in Fig.4, where the curve is drawn connecting average value using the cubic natural spline function.⁽⁷⁾ The profile of Fig.4 is obtained by data processing system especially developed for the present experiment.⁽⁸⁾ The emission coefficient or population density profile should be evaluated by the Abel inversion technique. In our case, however, assumption of cylindrical symmetry is largely violated due to high beta effect of the plasma by which the plasma is shifted away from the axis. Therefore we try to use non-cylindrical symmetric Abel inversion technique in which all data are divided into two parts, symmetric even parts and anti-symmetric odd parts. The most probable functions for symmetric parts are determined after Barr's method⁽⁹⁾ and the anti-symmetric odd parts by least square fitting. Although it is a difficult problem to estimate the error which appears in the emission coefficient, a reasonable guess may be in the range of average error contained in the intensity profile, since the emission coefficient is evaluated from the boundary value with a usual procedure which involve numerical differentiation and integration.

3. EXPERIMENTAL RESULTS AND EVALUATION OF NEUTRAL PARTICLE DENSITY

In the present operational condition of STP-2 the electron temperature falls in the range of 3-20 eV, while the density does $(1-20) \times 10^{14}/\text{cm}^3$. Figure 6 shows the electron density and temperature at 4.0 μsec . The electron density becomes small near the wall so that the density measurement by laser scattering is not possible. The electron density and temperature near the wall are estimated by extrapolating from their central parts like Fig.6. As can be seen simple Corona model may not be applicable because of too high density, so that electronic collisional de-excitation and direct ionization terms by electron impact should be important and we have following quasi-steady-state rate equations.

$$n_3 \cdot A_{3 \rightarrow 2} + n_4 A_{4 \rightarrow 2} + n_e \cdot \{n_3 F_{3 \rightarrow 2} + n_4 F_{4 \rightarrow 2}\} + n_e^2 \cdot \alpha(2) + n \cdot n_e \cdot C_{1 \rightarrow 2} - n_2 \cdot \{A_{2 \rightarrow 1} + r_e (C_{2 \rightarrow 3} + C_{2 \rightarrow 4} + F_{2 \rightarrow 1} + S(2))\} = 0, \quad (1)$$

$$n_4 \cdot A_{4 \rightarrow 3} + n_e \cdot n_4 F_{4 \rightarrow 3} + n_e^2 \alpha(3) + n_e \cdot \{n_1 C_{1 \rightarrow 3} + n_2 C_{2 \rightarrow 3}\} - n_3 \{A_{3 \rightarrow 1} + A_{3 \rightarrow 2} + n_e \cdot (C_{3 \rightarrow 4} + F_{3 \rightarrow 2} + F_{3 \rightarrow 1} + S(3))\} = 0, \quad (2)$$

where n_i is the population density of i -state of neutral deuterium and n_e the electron density, respectively. Further, the notations in Eqs.(1) and (2) are following:

$C_{i \rightarrow j}$: rate coefficient for excitation from level i to j by electronic collision.⁽¹⁰⁾

$S(i)$: that for ionization from level i .⁽¹¹⁾

- $A_{i \rightarrow j}$: Einstein coefficient for radiative transition from level i to j .⁽¹²⁾
- $\alpha(i)$: Rate coefficient for radiative recombination to level i .⁽¹⁰⁾
- $F_{j \rightarrow i}$: that for de-excitation from level j to i , and is equal to $C_{i \rightarrow j} \cdot \frac{\omega_i}{\omega_j} \cdot \exp\left(-\frac{E_{ij}}{T_e}\right)$.
- ω_i : statistical weight of level i .
- E_{ij} : excitation energy from level i to j .
- T_e : electron temperature.

Here unknown parameters are n_1 and n_2 . Knowledge of electron density and temperature permit the evaluation of all coefficients, while n_3 and n_4 are obtained by the present spectroscopic measurement of D_α and D_β .

In calculating the recombination terms $\alpha(2)$ and $\alpha(3)$ it is assumed that ion and electron densities are equal to each other due to quasi-neutrality of plasma and also that three body recombination must be very small for the present parameters. Plasma is called to be "in predominately ionizing state",⁽¹³⁾ where electrons flow mostly toward higher states and de-excitation processes are not so important. It is demonstrated in ref. 14 that plasma should be in such a state if the population density per unit statistical weight is proportional to i^{-6} in the case when the electron density is larger than $10^{12}/\text{cm}^3$ and the temperature is higher than $\chi_D/10$, where χ_D is ionization potential of deuterium. Actually the observed population densities per unit statistical weight are proportional to i^{-6} within experimental errors. Therefore, in Eqs.(1) and (2) the contributions from higher quantum states may be neglected without large errors in the present experiment.

Neutral particle density distributions thus obtained are shown in Fig.6, where the spatial resolution of electron density measurement are restricted by the slit height of the monochromator used in laser scattering

measurement, while the error bars attached to the value of electron density comes from data treated by the least square fitting analysis. The error bars given on the neutral density in the same figure are estimated from the assumption that electron temperature varies from -1 eV to +1 eV around the measured one with the other parameters kept constant. When electron temperature is lower than 10 eV, the excitation rate coefficient is a sensitive function of the electron temperature. It is of course that some errors of the neutral density arise from the errors contained in the electron density and the population density of the upper level population densities. As is seen from Fig.6(a) average ionization degree reaches up to about 50 % at 4 μ sec from the start of main discharge. Although very high ionization degree is achieved at the central part of plasma column where both electron density and temperature are also high, such a low average ionization degree is mainly due to many neutral particles which remain near the discharge tube wall. Plasma current distribution at this instant is observed to be relatively flat over the radius of 6 cm. As time goes on, average ionization degree also grows up and reaches almost 100 % at 8 μ sec. Figure 6(b) shows the neutral particle density distribution at 8 μ sec. It is noted that the peak electron density does not increase so much compared with the one at 4 μ sec. Improvement of average ionization degree comes from the ionization at plasma periphery, which consequently produces larger plasma density-radius. After 8 μ sec plasma keeps an approximately constant peak temperature of about 5 eV and density of $1.0 \times 10^{15}/\text{cm}^3$. It is also observed that the intensities of D_{α} and D_{β} show flat time evolution, which indicates that neutral particle density also is kept constant value. In other words plasma sets in steady-state after 8 μ sec. As is shown in Fig.7, the CO_2 laser interferometer measurement also confirms that plasma behaves as quasi-stationary state after 8

μsec . The total particle number contained in the discharge tube is the sum of neutral particles and electrons, which is obtained by spatial integration of density profiles in Fig.6. It agrees with the total gas particle number injected by the puff at initial phase within factor 2. This confirms that the present estimation of neutral particle density is considerably accurate.

4. DISCUSSION AND CONCLUSIONS

In this final section we discuss about the validity and limitation of physical model of the neutral particle density measurement written in the preceding sections.

As is described the population density of the state, $i = 3$ and 4 are obtained by the measured absolute intensities of D_α and D_β lines, and the quasi-steady state equations with respect to $i = 2$ and 3 are solved for the ground state population or neutral particle density. For the parameters of the present STP-2 operation the population density of $i = 2$ is strongly correlated only with its neighbors; $i = 1, 3$ and 4 and that of $i = 3$ does with $i = 1, 2, 4$ and 5 , since higher states remained may not be so important.⁽¹⁴⁾ Therefore information of $i = 5$ or D_γ intensity may help to improve the accuracy in solving the rate equations. However, influence of $i = 5$ on $i = 3$ may not be large compared with the error arisen from the Abel inversion or reproducibility of the present plasma. In this sense the intensities of D_α and D_β may give information enough to determine the neutral density. However, if only the intensity of D_α is measured and the neutral density is estimated from the calculation of branching ratio after corona model, this density has not a small error because of the lack of the excitation process from the level $i = 2$ to 3 .

In a tokamak experiments Lyman series lines are often used to estimate the ground state neutral particle density. Its observation includes difficulty in the case of high density like the present STP-2 or puff injected tokamaks⁽¹⁵⁾ because self-absorption problem becomes non-negligible. In Eqs.(1) and (2) the self-absorption by the radiation trapping effect of the ground state is not taken into account. The effect may become important for the large volume plasma system when its ground state population density is high and the electron density is lower than $10^{13}/\text{cm}^3$. Although the electron density of the present experiment is larger than $10^{14}/\text{cm}^3$, its influence on the preceding results is checked using the concept of the escape factor which modifies the Einstein coefficient $A_{i \rightarrow j}$. Actually the escape factor is a complicated function of a plasma shape, the population density of the ground state and the line profiles. It is tabulated in ref.16 as a function of optical depth. Since radiation trapping is a function of the unknown ground state density, iterative method has been tried to check whether it is important or not for the present results.

Starting with the density not taken any care of the effect, we find that it gives a solution with smaller neutral density by factor of 2 to 4 depending on the assumed model of plasma shape. This iterative treatment may over estimate the effect because for simplicity only Doppler effect is included to estimate the optical depth. However actual observation of line profiles of D_α and D_β by OMA (Optical Multichannel Analyzer) system shows that the line widths are at least twice as large as that expected by Doppler effect. The observed large line width may come from strong Stark effect which may be very important in this parameter range. It might be said that the ambiguity of factor of two may be absorbed into the assumed plasma model.

From physical point of view when the electron density exceeds $3.5 \times 10^{14}/\text{cm}^3$ the plasma is said to be in the quasi-saturation or complete-saturation state⁽¹⁴⁾ in which dominant ionization mechanism is provided by ladder-like excitation-ionization.⁽¹⁴⁾ When a plasma is in such a state collisional de-excitation dominates over other mechanisms like radiative decay processes which is largely influenced by radiation trapping, thus the treatment in the preceding section may be valid in high density operation.

The conclusion of this paper is that, neutral particle density in high density plasma was estimated using the absolute intensity of the Balmer alpha and beta lines with the techniques described in the preceding section. It is found that the neutral density is of the order of $10^{12}/\text{cm}^3$ in the center of plasma and $10^{14}/\text{cm}^3$ on the periphery. These values are about 100 times larger than those of a ordinary tokamak discharge, so that different treatment to estimate neutral particle density is necessary. The technique described here may provide a tool for the study of transport and ionization of hydrogen atoms in puff-injected high density tokamaks and may be also useful to investigate the fueling problem into a fusion reactor. Care must be taken of when it is applied to early phase of fast pinch experiments because the quasi-steady state approximation may not be applicable.

Acknowledgements

The authors thank Dr. T. Kato for her valuable discussions about the calculation of the rate equations. Very useful discussions and suggestions for hydrogen atomic physics given by Dr. T. Fujimoto is deeply acknowledged. They thank Professor T. Ishimura, Professor T. Amano and Professor M. Otsuka for helpful discussion. They also acknowledge Mr. H. Arimoto for his measurement of plasma density by CO₂ laser interferometer system and thank all the high beta group members of the Institute for their cooperations.

REFERENCES

1. H. Kraus, Vesh. Deut. Phys. Ges., No.7, 452 (1971).
2. G. Becker and D. F. Duchs, Plasma Phys. Suppl., 547 (1976).
3. G. Malesani, Proc. 2nd Topical Conf. Pulsed High-Beta Plasma, C2/87-90 (1972).
4. K. Hirano et al., Proc. 6th IAEA Conf., Tokyo, Vol.3, 463 (1974).
5. T. Matoba and A. Funabashi, Japan Atomic Energy Research Institute Report, JAERI-M6239 (1975).
6. K. Miyata and U. Yasumoto, to be published.
7. FACOM, SSL, Vol.2, 162 (1978).
8. S. Yamaguchi, to be published.
9. W. L. Barr, J. Opt. Soc. Am. 52, 885 (1962).
10. C. W. Allen, Astrophysical Quantities, 3rd ed. (1973).
11. T. Fujimoto, IPP-Nagoya Report, IPPJ-AM-8 (1978).
12. W. L. Wiese, M. W. Smith and B. M. Glennon, Atomic Transition Probabilities (National Standard Reference Data Series, National Bureau of Standards 4) Vol.I (1966)
13. T. Fujimoto, J. Phys. Soc. Jpn. 47, 265 (1979).
14. T. Fujimoto, J. Phys. Soc. Jpn. 47, 273 (1979).
15. M. Murakami, J. D. Callen and L. A. Berry, Nucl. Fusion 16, 347 (1976).
16. T. Holstein, Phys. Rev. 72, 1212 (1947).

Figure Captions

- Fig.1. Schematic drawing of STP-2 device and diagnostics around the torus.
- Fig.2. Waveforms of plasma current and toroidal field intensity.
- Fig.3. The spectroscopy system and its setting for the torus of STP-2.
- Fig.4. A line intensity profile of the Balmer-alpha and the population density profile of $i = 3$ at 4.0 μsec .
- Fig.5. The profiles of the electron temperature T_e and density n_e at 4.0 μsec obtained by ruby laser.
- Fig.6. (a) The profiles of an electron density n_e and a deuterium neutral density n_H at 4.0 μsec , the errors depend on the electron temperature (± 1 eV).
- (b) The same as (a) at 8.0 μsec .
- Fig.7. The time history of the line integrated electron density by the CO_2 -laser interferometer.

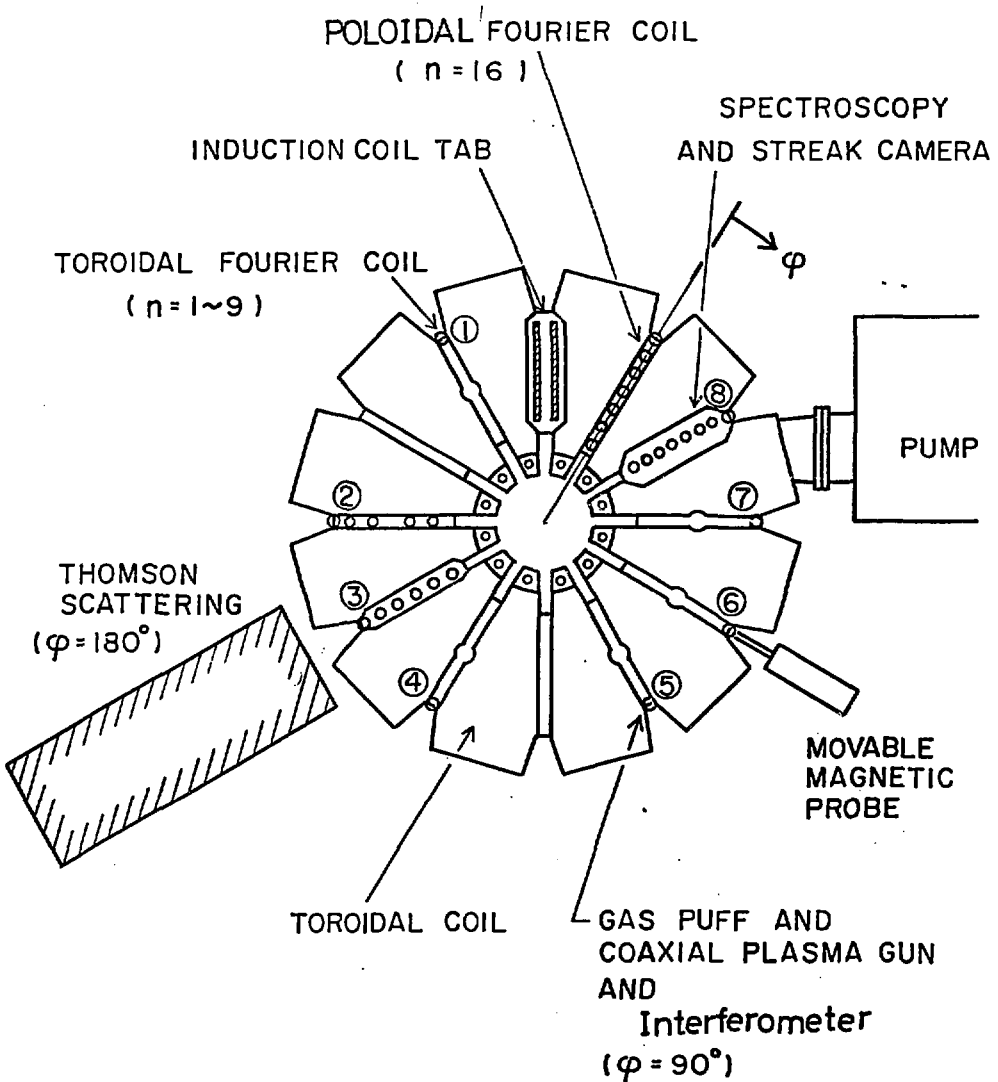


Fig. 1

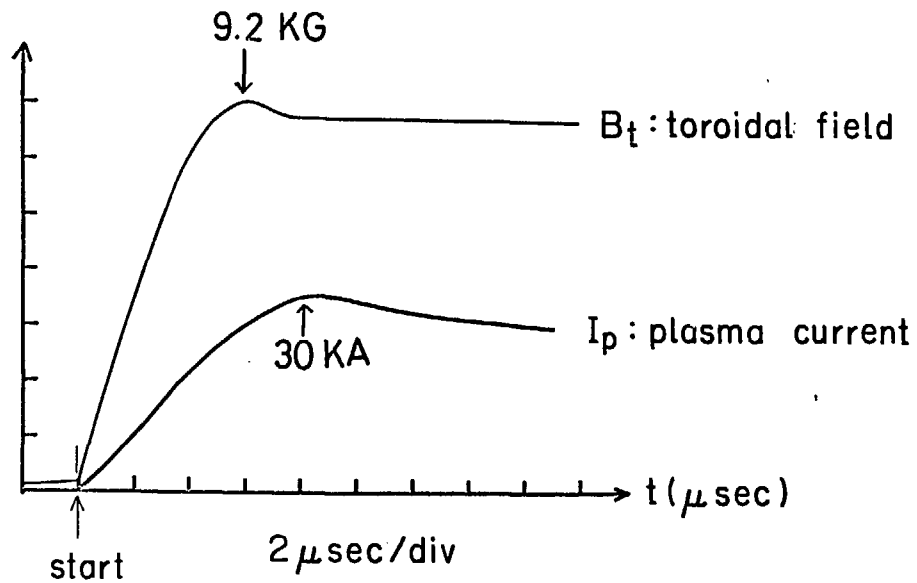


Fig. 2

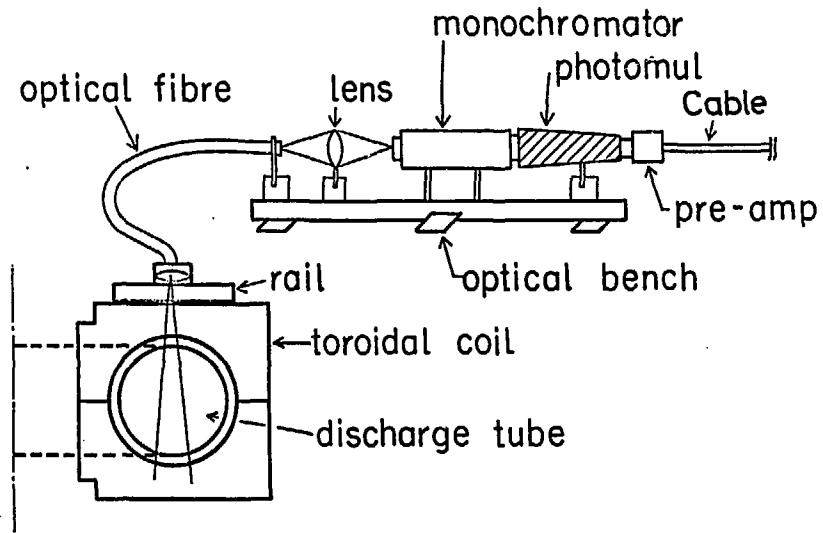


Fig. 3

$4.0 \times 10^5 \text{ erg/sec} \cdot \text{str} \cdot \text{cm}^2/\text{div}$

$3.00 \times 10^{10} / \text{cm}^3/\text{div}$

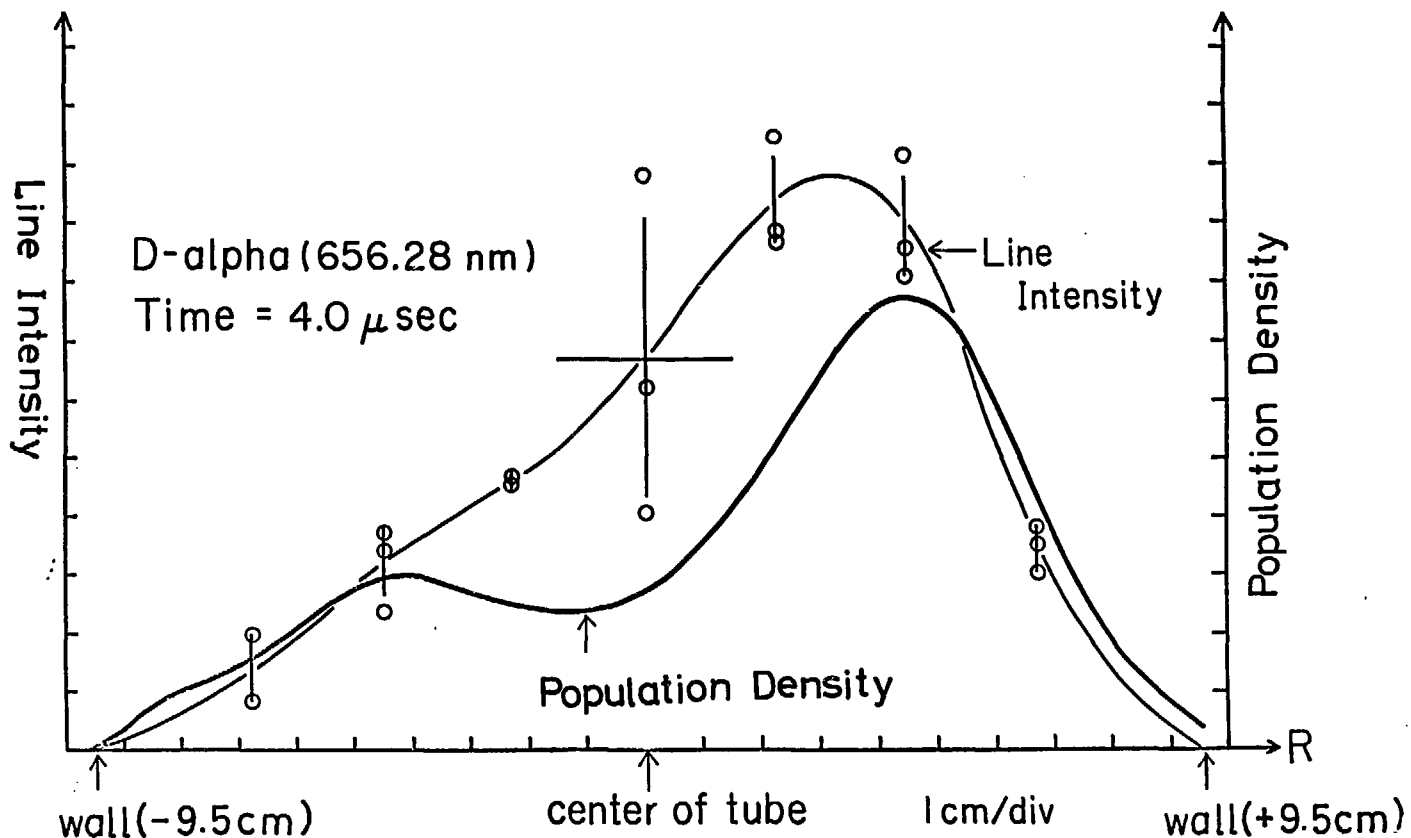


Fig. 4

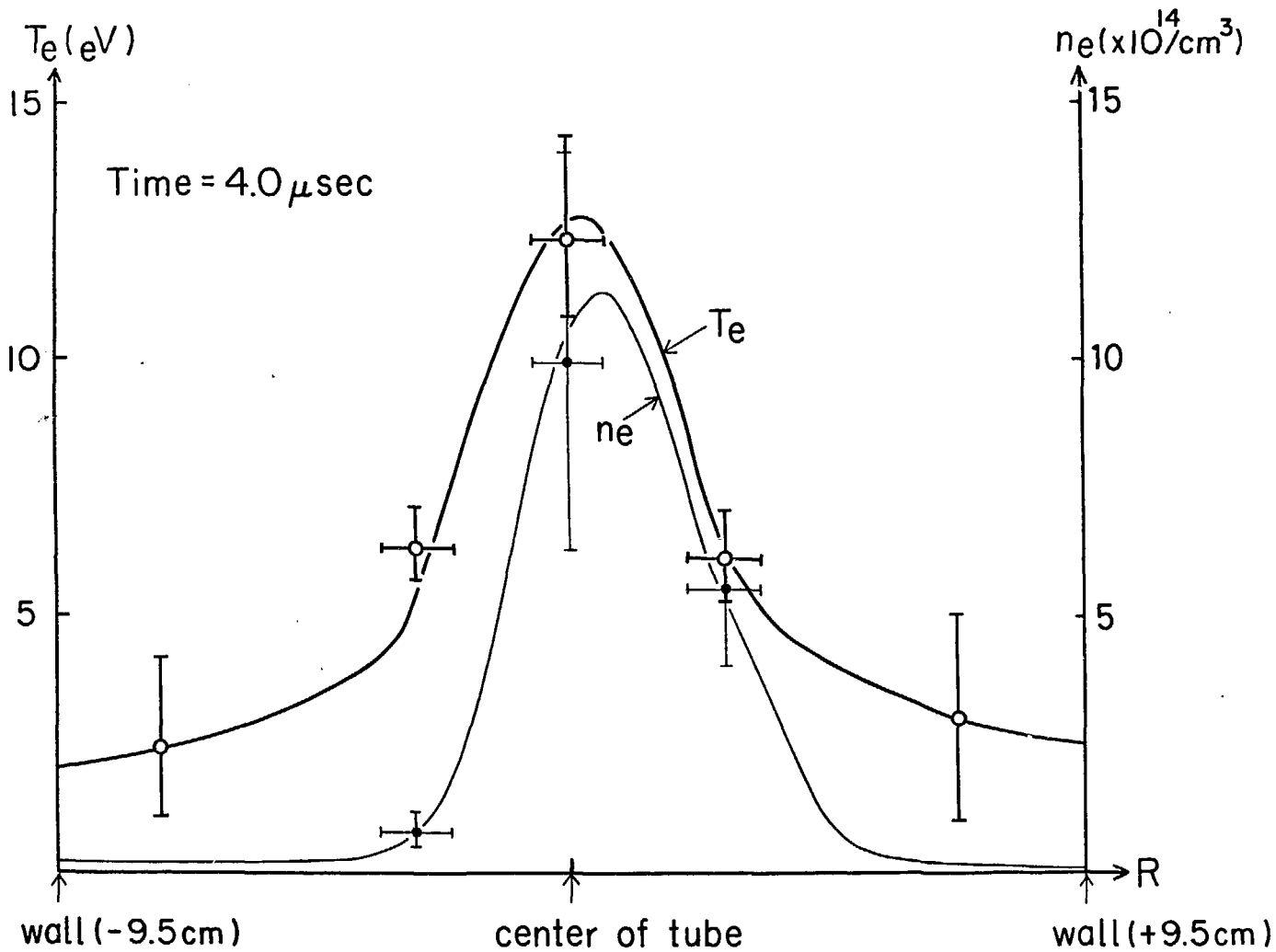


Fig. 5

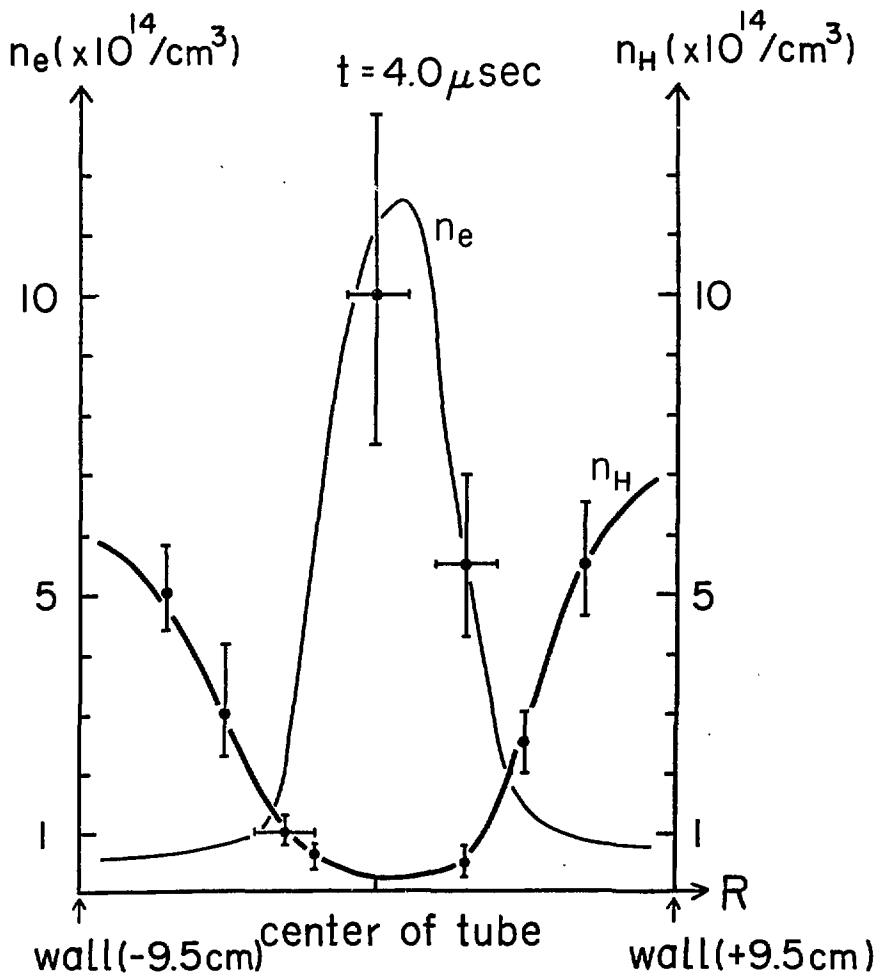


Fig. 6 (b)

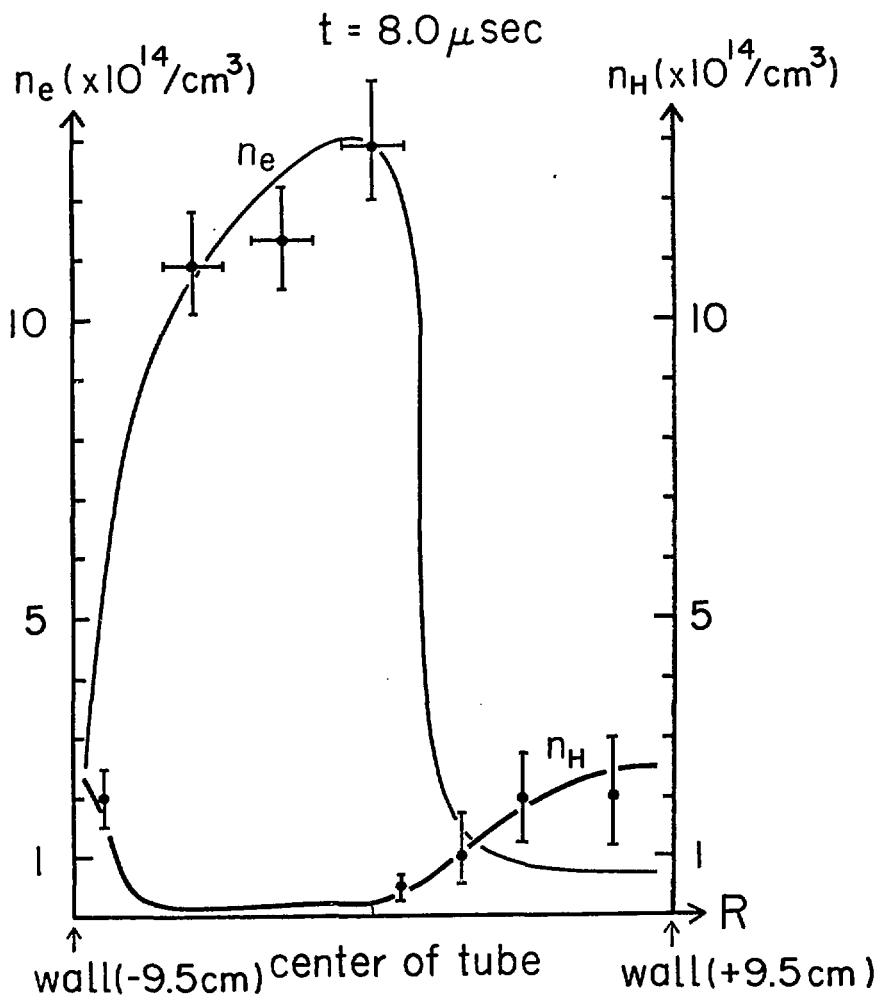


Fig. 6(b)

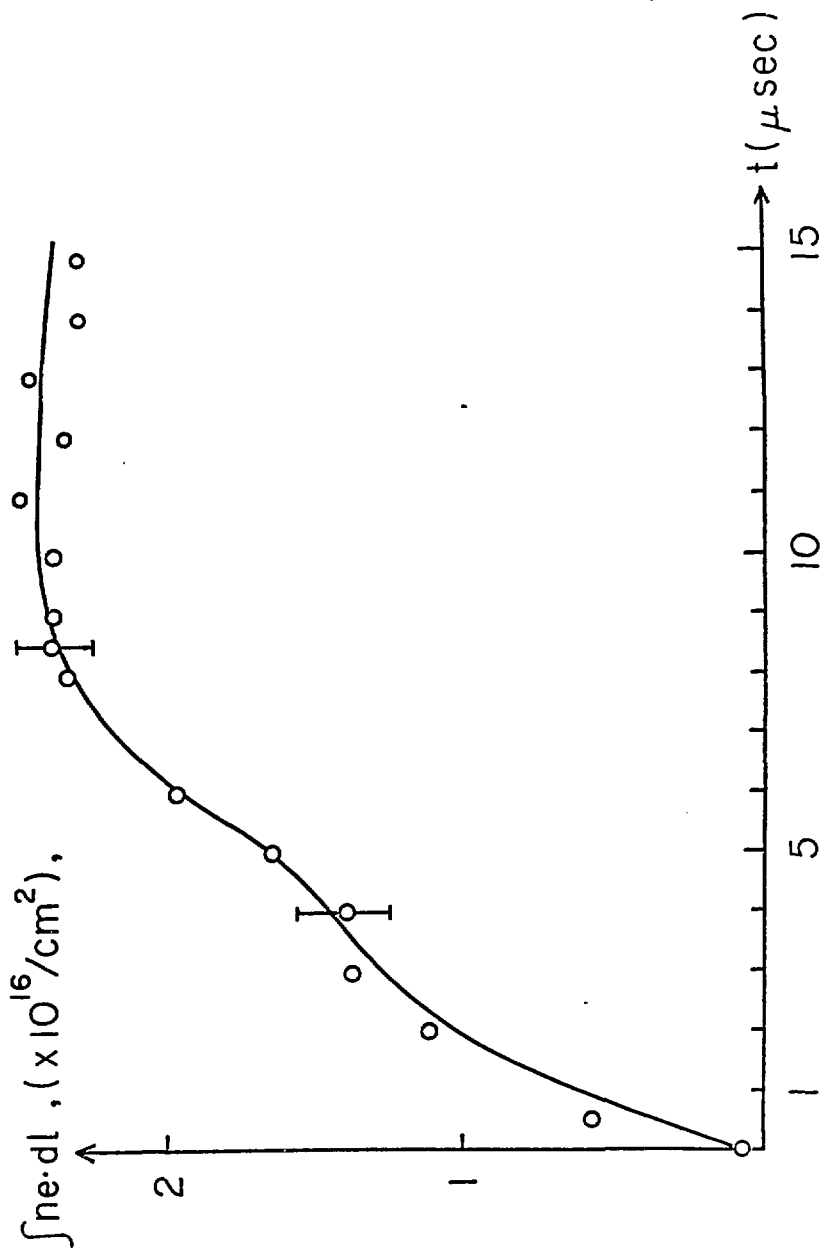


Fig. 7